Composition of agglomerates in fluidized bed reactors for thermochemical conversion of biomass and waste fuels Experimental data in comparison with predictions by a thermodynamic equilibrium model

Fuel (ISSN: 0016-2361)

Citation for the published paper:
Elled, A. ; Åmand, L. ; Steenari, B. (2013) "Composition of agglomerates in fluidized bed reactors for thermochemical conversion of biomass and waste fuels Experimental data in comparison with predictions by a thermodynamic equilibrium model". Fuel, vol. 111 pp. 696-708.

http://dx.doi.org/10.1016/j.fuel.2013.03.018

Fuel 111 (2013) 696–708

Contents lists available at SciVerse ScienceDirect

Fuel

journal homepage: www.elsevier.com/locate/fuel

Composition of agglomerates in fluidized bed reactors for thermochemical conversion of biomass and waste fuels Experimental data in comparison with predictions by a thermodynamic equilibrium model

A.-L. Elled [a], L.-E. Åmand [a,*], B.-M. Steenari [b]

[a] Chalmers University of Technology, Department of Energy and Environment, SE-412 96 Göteborg, Sweden
[b] Chalmers University of Technology, Department of Chemical and Biological Engineering, Industrial Materials Recycling, SE-412 96 Göteborg, Sweden

HIGHLIGHTS

- Well controlled full-scale tests in a fluidized bed boiler.
- The use of line-scans by the EDX spectrometer of the SEM on bed samples.
- Thermodynamic equilibrium modelling as a powerful tool in understanding the phenomena of bed agglomeration using quartz sand.

ARTICLE INFO

Article history:
Received 18 December 2012
Received in revised form 6 March 2013
Accepted 13 March 2013
Available online 10 April 2013

Keywords:
Fluidized bed boiler
Quartz sand
Alkali chlorides
Bed material
Agglomeration

ABSTRACT

Controlled combustion tests of biomass were performed in the 12 MWth circulating fluidized bed (CFB) boiler located on the campus of Chalmers University of Technology. The aim was twofold: to investigate the composition of agglomerated material and also to highlight the reasons for sintering and agglomeration during thermochemical conversion of biomass and wastes in fluidized bed reactors using quartz sand as bed material. Bed ash from three different tests regarding fuel or fuel mixtures (wood with straw, bark, and bark with refused derived fuel) was analysed to determine the ash elements using: (a) inductive coupled plasma (ICP) equipped with optical emission spectroscopy (OES) and (b) scanning electron microscopy equipped with an electron dispersive X-ray spectrometer (SEM–EDX). Chemical equilibrium calculations were also performed to support the interpretation of the experimental findings. It was found that the combination of (i) well controlled full-scale tests in a fluidized bed boiler, (ii) the use of line-scans by the EDX spectrometer of the SEM on bed samples and (iii) thermodynamic equilibrium modelling is a powerful tool in understanding the phenomena of bed agglomeration using quartz sand.

1. Introduction

Thermochemical conversion of biomass and waste-derived fuels for the production of heat, power and fuels used in the transportation sector are instrumental in the development of a sustainable society [1]. Biomass fuels are renewable and have the potential to be carbon dioxide neutral. The use of waste-derived material as fuel, as well as the disposal of waste by means of incineration, is expected to increase due to enforced legislation and the fact that the rate of waste generation is growing with population expansion. There are several environmental and socio economic benefits related to the above-mentioned energy carriers, but also technical challenges due to texture, chemical content and heterogeneity of the waste.

Fluidized bed reactors are well suited for thermochemical conversion of a wide range of biomass and waste fuels provided that the fuel can be given a suitable particle size. This technology is characterised by the bed which, in terms of combustion, is operated at relatively low temperatures, has a substantial heat capacity and is capable of tapping hazardous elements [2–5]. The capacity of the bed material to capture trace elements can be improved by adding clay minerals and/or limestone [6–9]. Further, fluidized bed reactors can handle mixes of fuels to evoke positive synergy effects with regard to the conversion process, reactor operation and emissions [10–12]. Biomass and waste derived fuels contain quite high concentrations of alkali metals, i.e. potassium and sodium. During heating, alkali metals are partly captured in the ash and partly released to the flue gas [13]. The main gaseous products pre-

* Corresponding author. Tel.: +46 31 772 1439.
E-mail address: lars-erik.amand@chalmers.se (L.-E. Åmand).

0016-2361/$ - see front matter © 2013 Elsevier Ltd. All rights reserved.
http://dx.doi.org/10.1016/j.fuel.2013.03.018

dicted by thermodynamic models are hydroxides (MOHs), sulphates (M_2SO_4), and chlorides (MCls) where M represents either K or Na, [14]. The formation depends on the access of chlorine and sulphur [13]. Alkali metal sulphates and, in particular, alkali metal chlorides have low melting temperatures and high vapour pressures [15]. Alkali metal compounds may deposit on the superheaters located in the exit- and/or convection section of the boiler. This can cause severe deposits and blockage of the flue gas pass in addition to corrosion of the superheater tube material. Ash may also deposit on surfaces exposed to predominantly radiant heat, e.g. furnace walls, subsequently causing so-called slagging [16].

A major problem in fluidised bed reactors for the conversion of biomass is sintering and agglomeration of bed particles, which prevent a proper fluidization and eventually result in the total collapse of the fluidised bed [19–29]. Both the terms agglomeration and sintering are used to describe the same phenomena. Sintering can be defined as the formation of bonds between particles at high temperatures [30] and is utilised in powder metallurgy in the production of items sustaining high temperature environments such as engine parts or turbine blades in steam- and gas turbines. An illustration of the high temperature sintering of a ceramic powder is shown in Fig. 1A. Agglomeration is defined as the formation of clusters of particles, i.e. agglomerates. In a fluidized bed reactor system, agglomeration and sintering of the bed material are associated with the formation of sticky coatings on bed particles. The coatings consist of multiple layers of ash or ash compounds. The

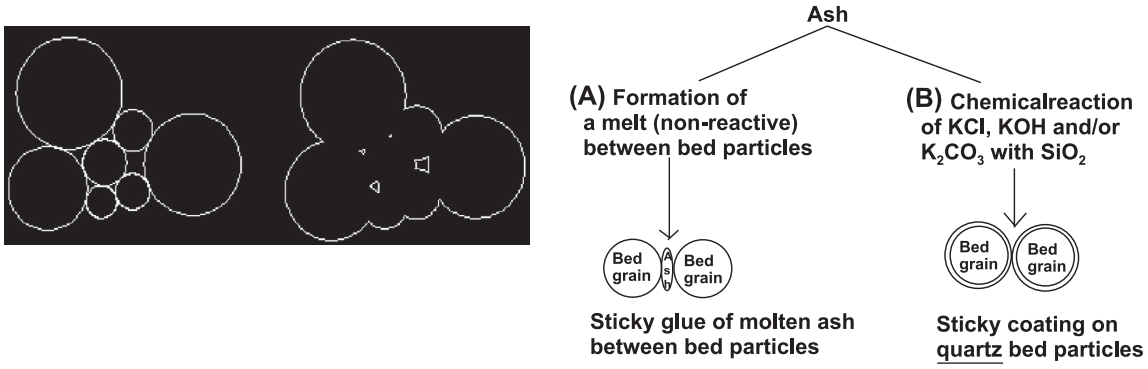

Fig. 1. (A and B) Theory of agglomeration/bed sintering of the bed material in fluidized bed systems using biomass.

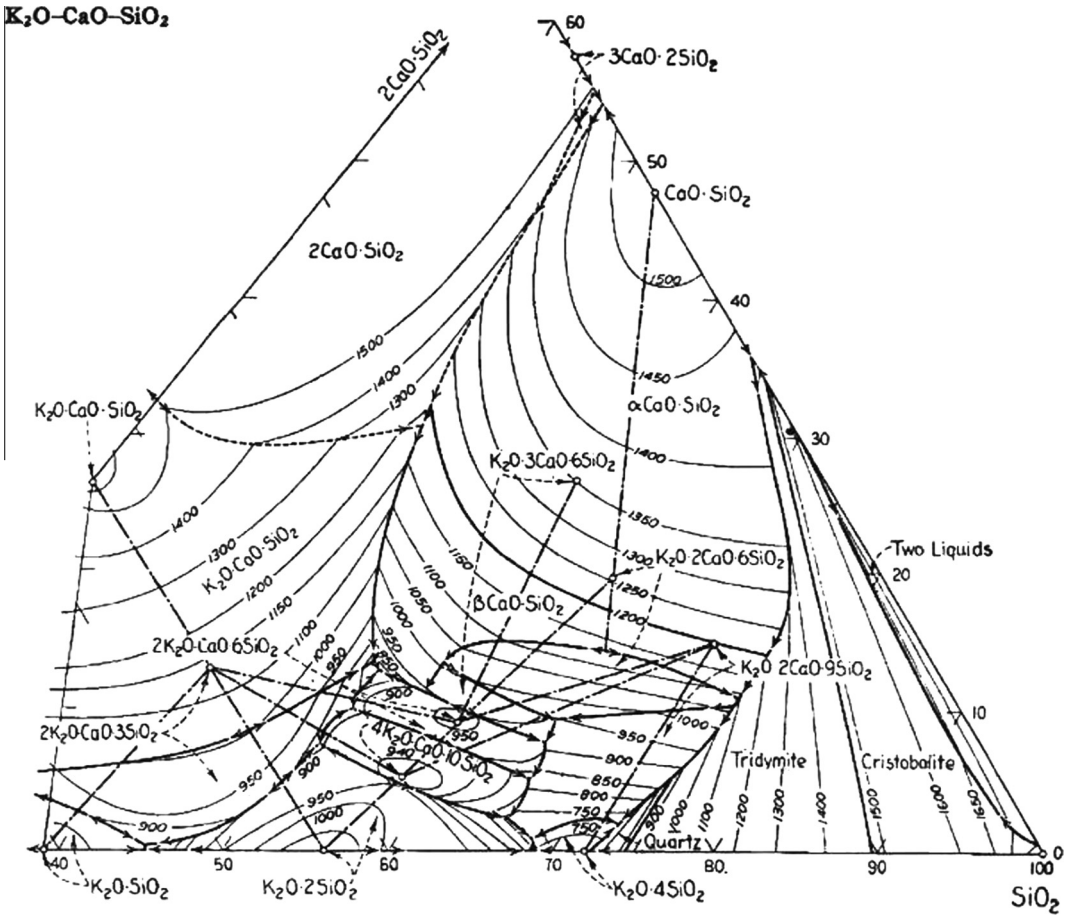

Fig. 2. The high SiO_2 corner of the phase diagram of the ternary system K_2O–CaO–SiO_2 [47,52].

Table 1
Experimental matrix.

	Unit	Case A wood–straw	Case B bark	Case C SRF/RDF
Load	MWth	6.4	6.7	6.7
Bed temp. (bottom)	°C	851	846	847
Comb. temp. (top)	°C	863	867	873
Comb. temp. after primary cyclone (5)[a]	°C	801	789	775
Flue gas temp. after bag filter	°C	152	151	145
Total riser pressure drop	kPa	7.4	7.4	7.7
Excess air ratio	–	1.26	1.21	1.20
Air staging: primary air flow divided by total air flow	%	57	55	54
Superficial velocity at the top of riser	m/s	4.9	5.8	5.9
S/Cl molar ratio	–	0.4	1.7	0.6
Cl/(Na + K) molar ratio	–	0.4	0.1	0.4
Co-fuel	% Dry fuel	26	0	21
Alkali loading	Mole/MWh	13.4	15.8	17.8

[a] At position 5 in Fig. 3.

Table 2
Fuel composition.

Fuel Test case	Wood pellets A	Straw pellets A	Bark pellets B and C	Solid recovered fuel C
Proximate analysis				
Water (wt.%, raw)	8.2	10.2	14.1	5.2
Ash (wt.%, dry)	0.2	5.0	4.7	12.8
Combustibles (wt.%, dry)	99.8	95.0	95.3	87.2
Volatiles (wt.%, daf)	81.7	80.7	73.2	88.4
Ultimate analysis (wt.%, daf)				
C	50.5	49.3	54.6	53.6
H	6.0	6.1	6.1	7.3
O	43.4	43.7	38.8	37.3
S	0.01	0.08	0.03	0.24
N	0.06	0.47	0.50	0.91
Cl	0.02	0.28	0.02	0.62
Ash analysis (g/kg dry ash)				
K	138	157	46	11
Na	7.5	6.3	10.3	22.2
Al	6.7	4.0	25.5	47.6
Si	36.5	230	110	138
Fe	8.8	3.4	12	17.9
Ca	152	72.4	198	192
Mg	29.8	12.2	17	11.4
P	13	12	10	5.1
Ti	0.4	0.1	1	10.6
Ba	2.2	0.7	2.9	1.8
Lower heating value (MJ/kg)				
Hu, daf	19.00	18.35	20.33	21.13
Hu, raw	17.71	17.09	19.43	17.77

daf = Dry and ash free, raw = as received.

inner layers appear to reflect the composition of the bed material whereas the outer layers appear to be more dependent on the ash characteristics of the fuel [17]. The formation of ash coatings and agglomeration has been subject to numerous studies and there are mechanisms suggested in the literature [17,18,23,26,27,31–33]. An attempt to describe the agglomeration phenomena with a simplified mechanistic model can be found in [34,35] and is used in [36] to explain the agglomeration during co-combustion of bark and rapeseed cake in a fluidized bed, Fig. 1B. This simplification lies in the division of the agglomeration process into two categories: mechanism A (see Fig 1B) in which a melt of ash is formed gluing the bed particles together [18] and mechanism B in which a reaction product is formed that connects the sand particles. Mechanism A acts on quartz particles as well as on bed particles that could be non-quartz like olivine sand or originating from blast furnace slag [37,24]. Mechanism A is a non-reacting mechanism where the fuel ash has a composition that melts at the operating temperature of the fluidized bed and this melt becomes sticky and acts as a glue for the bed particles regardless of the composition of the bed material. The melt could be straw ash rich in silica and consist of potassium silicates or ash from rapeseed cake and then consist of potassium–calcium–phosphates, [38,39]. Mechanism B in Fig. 1B is a reacting mechanism where the ash layer formation is initiated when: (i) gaseous, liquid and/or aerosol potassium compounds (KCl, KOH, and K_2SO_4) [14] react with the quartz (SiO_2) bed material in (ii) combination with diffusion and/or dissolving of calcium into the melt [17,25–28,33,34] where calcium can react with the melt forming calcium–potassium silicates which is non-sticky at normal operating temperatures of a fluidized bed boiler (800–900 °C) burning biomass. The calcium content of the biomass thereby becomes important as in bark [24] since it can decrease the sintering process caused by the alkali metal salts. Regeneration of the quartz bed material, which replaces the coated quartz sand with fresh sand, is a commonly used strategy to avoid bed agglomeration in fluidized bed boilers [37]. Adding limestone to cover the quartz sand grains is another useful strategy that was first discovered in the project published in [38] and thoroughly analysed in [40].

The case of operation with quartz sand (SiO_2) as bed material is given in reaction (R1) and (R2) exemplified with KOH and NaOH as an alkali source in gas phase alkali causes agglomeration by reacting with the quartz (mechanism B) and forming eutectic mixtures with low melting temperatures as can be seen for $K_2O{\cdot}4SiO_2$ in the high SiO_2 corner of the phase diagram system K_2O–SiO_2–CaO, Fig. 2.

$$4SiO_2(s) + 2KOH(g) \rightarrow K_2O \cdot 4SiO_2(l) + H_2O(g) \quad (R1)$$

$$2SiO_2(s) + 2NaOH(g) \rightarrow Na_2O \cdot 2SiO_2(l) + H_2O(g) \quad (R2)$$

Several ash elements, such as Al, Ca, Fe and Mg, and compounds are known to improve the melting behaviour of a bed material rich in alkali metal compounds, thus decreasing the agglomeration tendency of the bed. All current preventive measures are based on changing the average chemical composition of the bed material by co-firing different fuels to obtain a more favourable composition of the ash, adding sorbents to the bed or changing the bed material.

Kaolin ($Al_2O_3{\cdot}2SiO_2{\cdot}2H_2O$) has been identified as one of the most efficient sorbents for sequestration of potassium [37,42–44]. Kaolin reacts with potassium containing species to form both amorphous and crystalline phases with high melting points.

Reactions (R3) and (R4) describe the formation of kalsilite ($KAlSiO_4$) and leucite ($KAlSiO_6$) found in ash from combustion of straw when kaolin was added [42].

$$Al_2O_3 \cdot 2SiO_2 \cdot 2H_2O + 2KCl \rightarrow 2KAlSiO_4 + H_2O + 2HCl \quad (R3)$$

$$Al_2O_3 \cdot 2SiO_2 \cdot 2H_2O + 2SiO_2 + 2KCl \rightarrow 2KAlSiO_6 + H_2O + 2HCl \quad (R4)$$

The presence of Fe_2O_3 can reduce the risk of agglomeration since it reacts with alkali present in the bed according to reactions (R5) and (R6) and form eutectic mixtures with melting temperatures exceeding 1135 °C [20]. The reaction makes alkali metals less available for reactions with quartz.

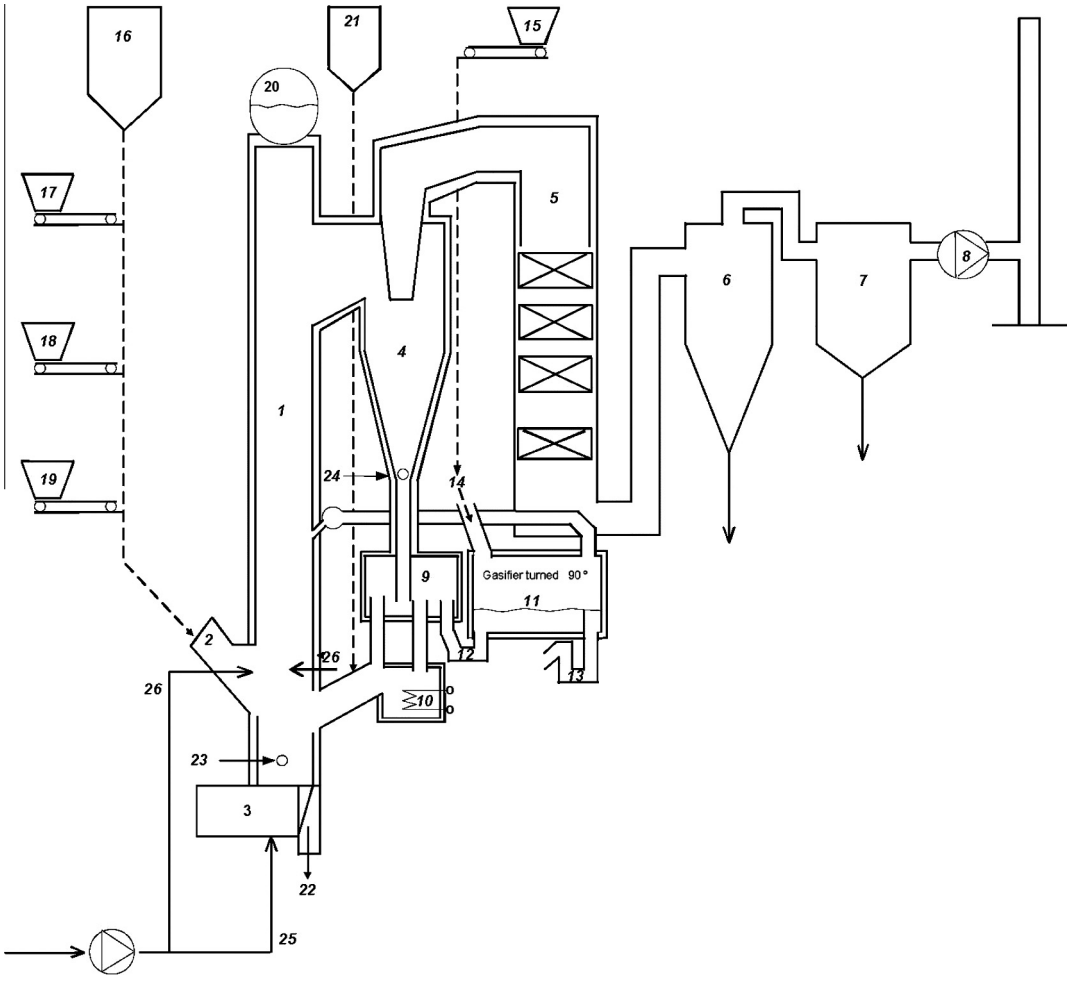

Fig. 3. Overview of the Chalmers CFB research boiler facility with the gasifier included. (1) furnace, (2) fuel feeding to furnace, (3) wind box, (4) cyclone, (5) convection pass, (6) secondary cyclone, (7) bag house filter, (8) flue gas fan, (9) particle distributor, (10) particle cooler, (11) gasifier, (12) particle seal 1, (13) particle seal 2, (14) fuel feeding (gasifier), (15) fuel hopper (gasifier), (16) hopper for bed material (quartz sand), (17) fuel hopper 1, (18) fuel hopper 2, (19) fuel hopper 3, (20) steam drum, (21) hopper for additive to bed material, (22) ash removal, (23) position for bed sample. (24) position for cyclone leg sample, (25) primary air flow, and (26) secondary air flow.

$$Fe_2O_3 + M_2O \rightarrow M_2Fe_2O_4 \quad (R5)$$

$$Fe_2O_3 + M_2CO_3 \rightarrow M_2Fe_2O_4 + CO_2 \quad (R6)$$

Further examples of materials and elements found to increase the melting points of ash to temperatures higher than those normally encountered in fluidised bed reactors include dolomite ($CaCO_3{\cdot}MgCO_3$), olivine ($(Mg, Fe)_2SiO_4$), blast-furnace slag (a by-product of iron and steel-making with high content Si, Ca and Mg) [37,44,45]. The involvement of calcium and magnesium in ash compounds tends to result in a general increase of the melting temperature [42].

The aim of this work was to investigate the composition of agglomerated material and further highlight the reasons for sintering and agglomeration during thermochemical conversion of biomass and wastes in fluidized bed reactors. Advanced thermodynamic modelling is an important tool used in the present paper in addition to investigations of samples from combustion experiments. A recent review on this topic [15] states that: *"The K_2O–CaO–SiO_2 system which is important for slagging and agglomeration in biomass combustion still needs experimental investigations to make accurate modelling possible."* For this purpose the research boiler, the 12 MW circulating fluidised bed (CFB) boiler at Chalmers University of Technology was used in well controlled tests using various kinds of biomass and waste fuels. This in turn imposed the risk of agglomeration and even the complete collapse of the operation of the boiler due to the full development of agglomerates in the particle distributor of the boiler.

2. Experimental

2.1. Research boiler and operating conditions

The work presented in this paper was part of an extensive research program including combustion issues, ash sintering and alkali metal chemistry as well as investigations of super heater corrosion [5–7]. Fig. 1 shows a schematic sketch of the 12 MW CFB boiler used. The boiler was built for research purposes and has all the characteristic features of a small scale boiler for the production of heat and power. Fig. 2 shows a schematic picture of the facility. The combustion chamber (1) has a cross section of 2.25 m^2 and a height of 13.6 m. The various fuels are fed to the bottom of the bed through fuel chutes (2). The circulating material is separated at a primary cyclone (4) and returned to the combustion chamber through the cyclone leg (24) and particle seal (9). An external heat exchanger (10) cools the circulating material before re-entering the combustion chamber when required. The boiler

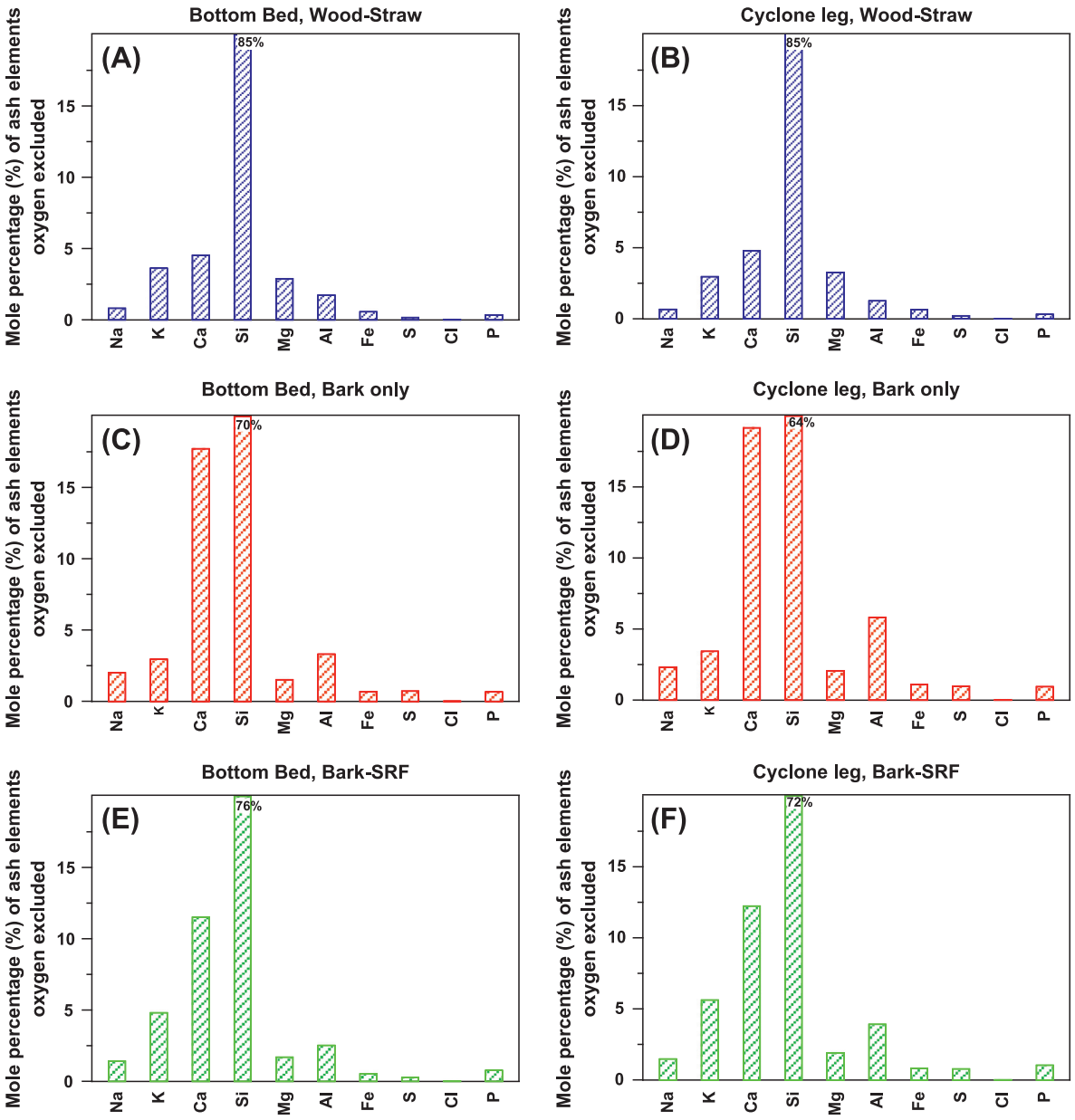

Fig. 4. (A–F) Mole percentage (%) of ash forming elements, (except oxygen) in bulk bed samples taken in the bottom bed and cyclone leg, nos. 23 and 24 in Fig. 3.

can also be operated in gasification mode by circulating the bed material through the gasifier (11), feeding fuel to the gasifier (14, 15) and fluidizing the gasifier with steam. Primary air is introduced through air nozzles located at the bottom of the riser and secondary air 2.2 m above the bottom plate. The exhaust gas is cooled to 150 °C in the convection pass before the fly ashes are separated in the secondary cyclone (16) and the textile filter (17). Silica sand (dp = 0.3 mm) was used as bed material in all tests. The operating conditions presented in Table 1 are typical of a commercially operated CFB boiler. This means a fluidizing velocity of approx. 5 m/s in the top of the riser that leads to a proper circulation of bed material through the primary cyclone, good heat transfer of moving bed particles and an attrition of the fuel ash into fly ash. This is important if accumulation of fuel ash in the bed is to be avoided. Typical operating conditions are also proper excess air ratio (20–25% excess air) and combustion temperatures above 850 °C for a residence time of more than 2 s in order to fulfill the requirements set for burning waste (within the European Union [21]).

2.2. Experimental procedure

Table 1 shows the experimental matrix. Three combustion tests are included in this work. In test case A, straw pellets produced from wheat were co-fired with biomass consisting of sawdust pressed into pellets (hereafter called wood pellets). The fuel mixture was composed of 74% wood pellets and 26% straw pellets based on mass of dry fuel. The share of straw was estimated to generate a sufficiently problematic fuel to induce sintering and bed agglomeration during the experiments and a total shut down if run for a period of one week with no regeneration of the bed material. In test B, Swedish forest residues consisting of crushed and dried bark pressed into pellets were fed to the reactor. In test C, these bark pellets were co-fired with fuel pellets produced by Ico-Power in the Netherlands. This fuel is also sold under the name refuse derived fuel (RDF) and it consists of combustible matter such as paper, wood, textiles and plastic. This is sorted waste that has been crushed and pressed into pellets. The fuel mixture was com-

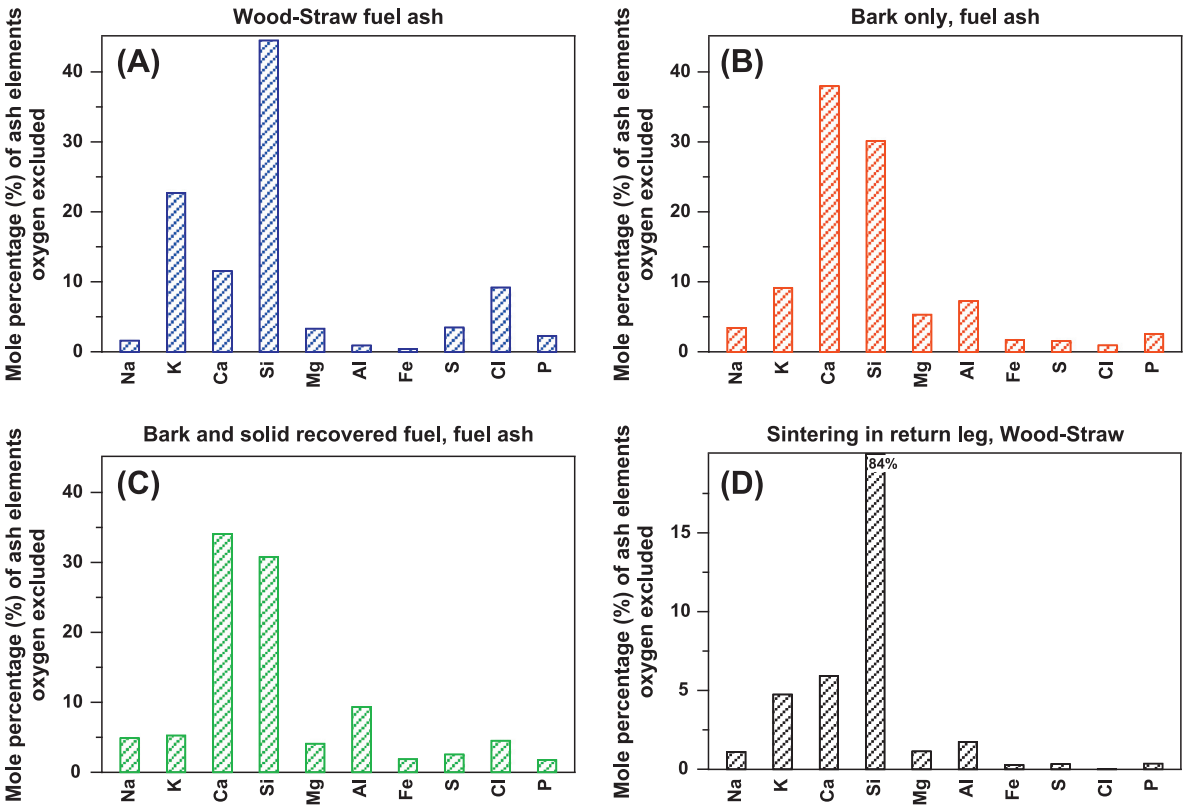

Fig. 5. (A–D) Mole percentage (%) of ash forming elements, (except oxygen) in fuel ash fed to the boiler during the three test series (A), (B) and (C), and in a sintered agglomerate taken in the return leg (D).

Fig. 6. (A and B) Agglomeration of the bed material found in the particle distributor, 9 in Fig. 3.

posed of 79% bark pellets (denoted BP) and 21% RDF pellets (denoted SRF) based on a mass of dry fuel.

The ash samples investigated in this work were collected both at the bottom of the bed and from the cyclone leg. The cyclone leg position normally suffers severe agglomeration and plugging using fuels rich in alkali metals. The material agglomerated was collected from the particle seal. The bottom bed samples are denoted BB and the cyclone leg samples CL.

2.3. Fuel composition

Table 2 shows the composition of the fuel. Wood pellets (WPs) is a well-defined and high quality fuel easy to handle and process. The content of combustibles is high and the presence of alkali metals and chlorine low. Straw pellets (SPs) is a more challenging fuel to combust due to its combination of content of alkali metals chlorine and silicon. By mixing the straw with wood, the alkali loading can be kept at the same order of magnitude as when using 100% bark pellets, Table 1. Bark pellets (BPs) contain less alkali metals and chlorine compared to straw pellets and a higher concentration of aluminium and calcium. Solid recovered fuel (SRF) is relatively dry which gives a comparably high heating value but with high content of chlorine and ash. Burning SRF also increases the loading of calcium compared to the Straw–Wood Case (A).

2.4. Experimental procedure

The main element concentrations in bed materials and ash samples were determined after total dissolution by an ICP-OES analyser (Inductive Coupled Plasma equipped with an Optical Emission Spectroscopy detector).

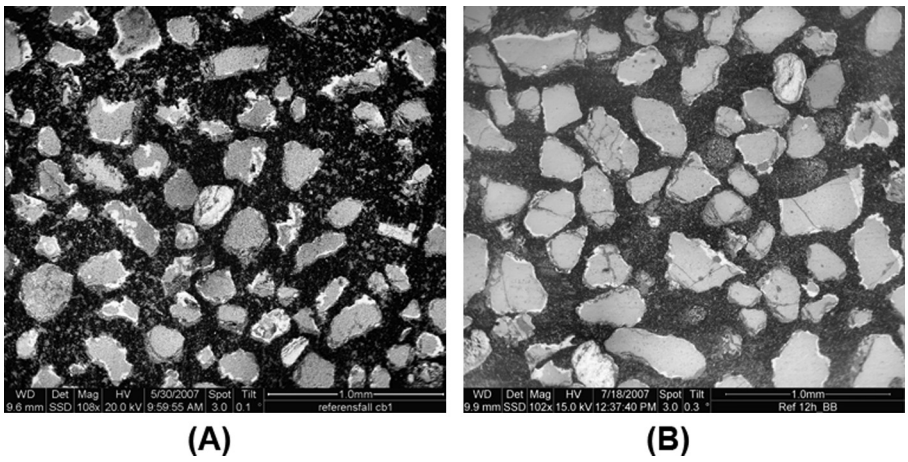

Fig. 7. (A and B) Back scattered electron images of bed sand particle cross-sections for test A: a mixture of wood and straw pellets. The image to the left shows bed material taken from the cyclone leg (CL) and the image to the right shows ash from the bottom bed (BB).

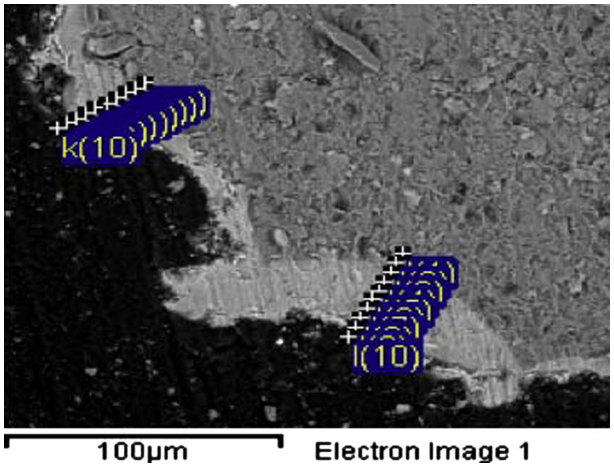

Fig. 8. Ash coating on the surfaces of a quartz particle in ash from the cyclone leg (test case A, straw and wood, cyclone leg sample).

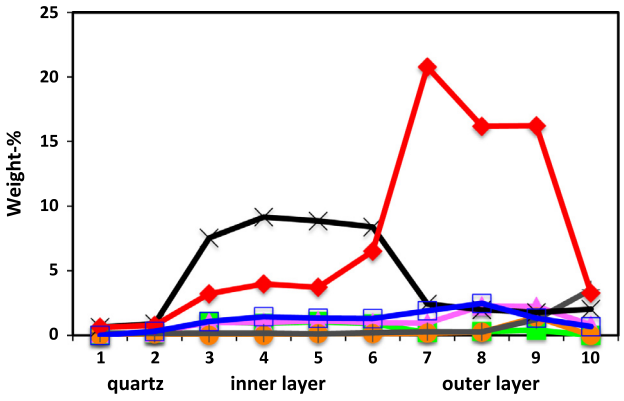

Fig. 9. Elemental concentrations (wt.-%) in each spot of the line scan "K" in Fig. 8. Spots 1 and 2 is the quartz particle. Spots 3–5 represent the inner ash layer, spots 7 and 8 the outer ash layer and spots 9 and 10 the border between the outer layer and the epoxy resin. Silicon and oxygen excluded in the plot.

Both the presence of ash layers on the bed material particles and the distribution of elements in the ash layers were studied using scanning electron microscopy (SEM) with energy dispersive X-ray fluorescence measurements coupled set on low vacuum mode. The specimens were prepared by embedding the sample in epoxy resin and grinding the surface to expose cross-sections of a sufficient amount of representative particles. SEM micrographs were taken with a Solid State Detector in the back scattered electron mode to obtain an overview of the differences in density.

2.5. Thermodynamic equilibrium modelling

Advanced thermodynamic equilibrium modelling has become a widely used method [15,17,26,45,46,48,53] it is an important tool for studying high temperature processes and ash-forming elements in biomass and waste combustion and gasification [26,41,49–51]. The method is fast and cost effective. However, it also has some drawbacks. Thermodynamic equilibrium modelling neither accounts for physical phenomena and local conditions, nor for reaction kinetics. One major limitation is the lack of consistent databases that contain the thermodynamic data of ash compounds and phases formed during heating and combustion. It is important to consider these shortcomings when evaluating the results.

The computer program FactSage version 6.2 and the module EQUILIB were used in this study and the thermodynamic data was collected from the database FTsalt, FToxid and FACT53 [15]. The calculations were performed for temperatures from 600 to 1200 °C at 1 atm. The ash-forming elements included in the model were K, Na, Ca, Mg, Fe, Al, Si, P, S, Cl together with C, H, O. As input to the model, the results of the SEM–EDX analysis on the bed particles are used which is unlike the practice in previous work by other research groups. For example, in the work by Öhman et al. [26] the ash analysis of the fuels was used as input to FactSage version 5.2. SEM–EDX analysis of coatings on bed particles was used in the study in [17]. However due to lack of thermodynamic data for the K_2O–CaO–SiO_2 system, data from the ternary phase diagram K_2O–CaO–SiO_2 [52] was used as a complement. Since then the FToxid database of the FactSage version 6.2 has been optimised and therefore used in the present paper for the prediction of ash chemistry and the melting behaviour of ashes within the fluidized bed environment using quartz sand as bed material.

3. Results

3.1. Ash forming elements

Fig. 4A–F shows the element composition determined by ICP-OES of the bed material samples taken in the bottom bed and cy-

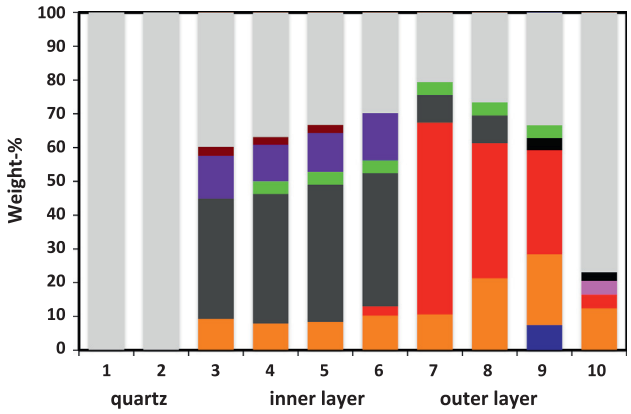

Fig. 10. The calculated equilibrium compositions in each spot of the line scan (mass%). Spots 1 and 2 is the quartz particle. Spots 3–5 represent the inner ash layer, spots 7 and 8 the outer ash layer and spots 9 and 10 the border between the outer layer and the epoxy resin.

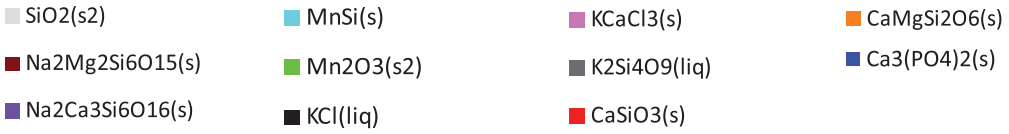

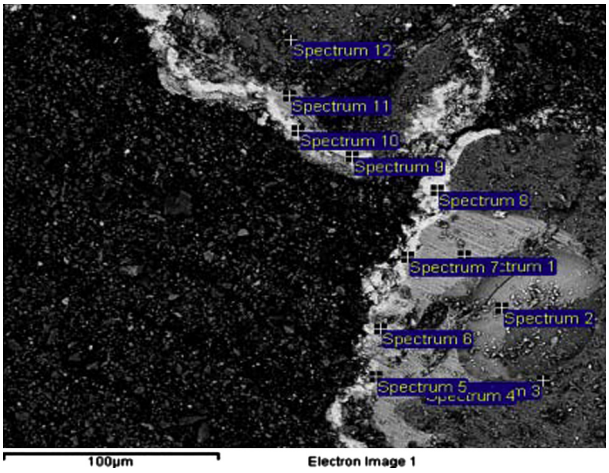

Fig. 11. Ash coating on the surfaces of two quartz bed particles taken from the cyclone leg (test case B, bark pellets).

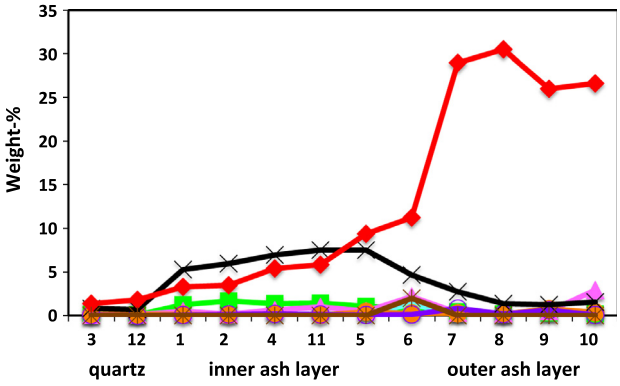

Fig. 12. Elemental concentrations (wt.-%) in each spot of Fig. 11. Spots 3 and 12 is the quartz particle. Spots 1, 2, 4, 11 and 5 represent the inner ash layer, and spots 7–9 the outer ash layer. Silicon and oxygen excluded in the plot.

clone leg for the three test cases. The result reflects the fuel ash composition in Table 2 and clearly seen in Fig. 5A–D. The bulk bed samples are dominated by Si originating from the quartz bed material. Due to reaction of ash elements with the quartz, a spectrum of elements is seen in Fig. 4A–F. The total content of alkali, i.e. the sum of K and Na, is between 5 and 7 mol-%. The most prominent difference between the sample compositions shown in Fig. 4A–F is the Ca content. In case A (wood straw) 5 mol-% of Ca was found while in the bark case B a Ca content of almost 18 mol-% was reached. The reason for this is clearly seen in Fig. 5B showing the ash forming elements for bark with a Ca concentration of almost 40 mol-%. The concentration of Cl is very low in all samples taken in the bottom bed and cyclone leg (Fig. 4A–F) since it has been released into the gas phase as alkali chlorides and hydrogen chloride (HCl). Fig. 5D shows the mole percentages of the elements selected in sintered agglomerate taken in the return leg. The composition of this sample resembles that of the cyclone leg sample taken for the wood-straw case where there is a lack of Ca to prevent agglomeration (Fig. 4A). The agglomerate was created and built up in the cyclone leg (No. 24 Fig. 3) but collected on the particle distributor represented by No. 9 in Fig. 3. Fig. 6A is a picture from this location during a shutdown of the boiler caused by severe problems with agglomeration of the bed material. The agglomerated material is shown in Fig. 6B.

3.2. Case A: wood pellets and straw pellets

Fig. 7A and B shows an example of the back scattered electron images of the samples obtained with the SEM. The bed material samples were taken from the cyclone leg (left image) and the bottom bed (right image) during combustion of wood and straw pellets (test case A). The images give an overview of a number of bed particles in each sample. Note the scale of 1 mm at the bottom corner of each image. The mean average size of the quartz sand used as bed material is 0.3 mm which fits suitably into the sizes seen in Fig. 7A and B. The ash layers around the quartz sand particles are in general sintered and denser compared to the quartz sand and are visible as a bright coating on the bed particle surface. It can be concluded that ash coatings on bed particles frequently occur when wood and straw pellets are burned in a fluidized bed boiler.

To investigate the ash layers more closely, attention was directed towards a number of particles representative for the whole ash sample. Fig. 8 shows a cross-section of such a particle coated with

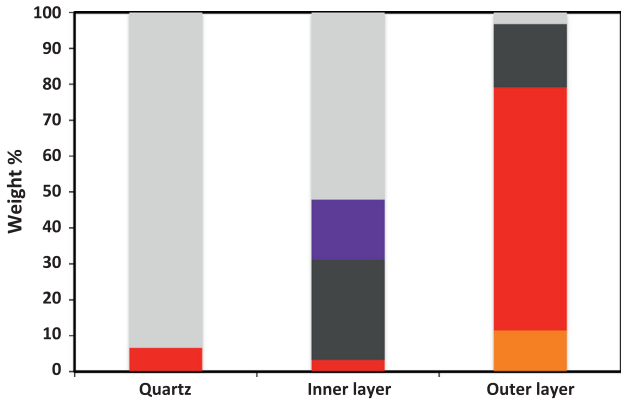

Fig. 13. The calculated equilibrium compositions in each of the three groups; the core of the bed particle (quartz), the inner, and the outer ash layer (wt.-%).

SiO2(s2) Na2Ca3Si6O16(s) K2Si4O9(liq) CaSiO3(s) CaMgSi2O6(s)

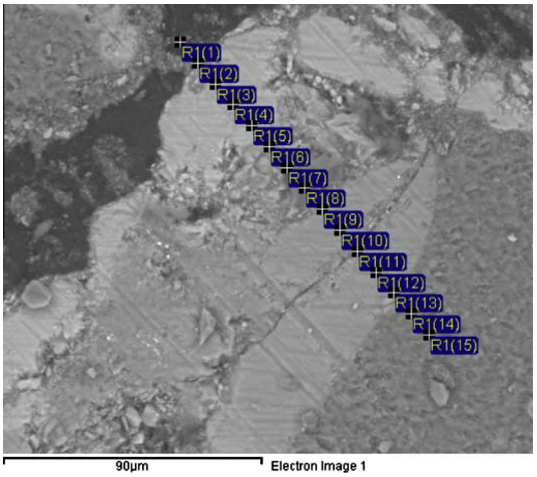

Fig. 14. Bed particle with ash layer. Test case C, bark pellets an solid recovered fuel, bottom bed sample).

an ash layer. The dark grey area is the quartz sand particle and the lighter grey coating on the particle surface is the ash layer. The black area is the epoxy resin. A close look at the ash layer shows that it is heterogeneous and a thin shell composed of denser material (inner ash layer) can be distinguished from an outer ash layer (lighter shades of grey). The quantification of elements along the line scans was obtained by EDX. The detection limit for the EDX analysis is 1% by weight. Fig. 9 shows the elemental composition at the ten positions marked reaching from the core of the quartz particle to the outer layer of the coating.

The result shows that the coating can be divided into an inner, and an outer ash layer. The inner layer is rich in K and contains Ca together with low concentrations of Mg, Na and Mn. The outer layer is rich in Ca. The concentration of Mg and Mn is increased somewhat while the amount of K is decreased.

The equilibrium composition together with the state of the composition (solid or liquid state) was modelled in each spot of the line scan. Fig. 10 shows the results at 850 °C. Spots 1 and 2 represent the quartz particle, spots 3–5 the inner layer and spots 7–8 the outer ash layer of the coating. These positions (spots 7–8) are too far out in the epoxy to give representative results related to the outer ash layer. The inner layer is predicted to be composed of both solid and liquid compounds. Sodium is thermodynamically stable either as $Na_2Mg_2Si_6O_{15}$ or $Na_2Ca_3Si_6O_{16}$. The most probable stable form of manganese is Mn_2O_3 Ca is present as $CaMgSi_2O_6$ or $CaSiO_3$. The inner layer is composed of almost 40% liquid potassium silicates ($K_2Si_4O_9$). The composition of the inner ash layer is likely to initiate sintering and induce agglomeration.

The dominating ash compounds in the outer layer at 850 °C are, apart from SiO_2, $CaSiO_3$, $CaMgSi_2O_6$ and Mn_2O_3. The amount of liquid $K_2Si_4O_9$ falls to only 8%, 1/5 of the value in the inner layer (spots 7 and 8).

3.3. Case B: bark pellets

Fig. 11 shows the cross-section of two quartz particles from the cyclone leg sample collected during combustion of bark pellets. Both particles are clearly coated with ash. The differences in grey-

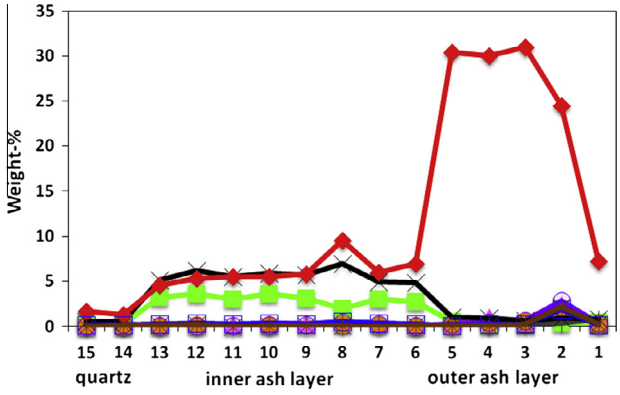

Fig. 15. Elemental concentrations (wt.-%) in each spot of Fig. 14. Spots 15 and 14 is the quartz particle. Spots 13–6 represents the inner ash layer, and spots 5–3 the outer ash layer. Silicon and oxygen excluded in the plot. Na Mg Al P S Cl K Ca Mn Fe

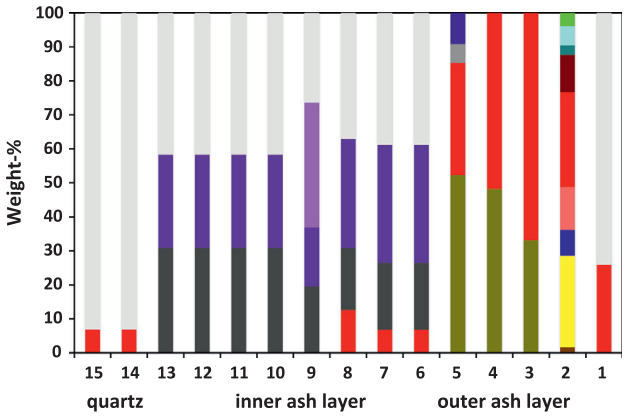

Fig. 16. The calculated equilibrium compositions in each spot of the line scan (wt.-%) of Fig. 15. Spots 15 and 14 is the quartz particle. Spots number 13–6 represents the inner ash layer, and spots 5–3 the outer ash layer. Spots 1 and 2 are positioned in between outer layer and epoxy resin.

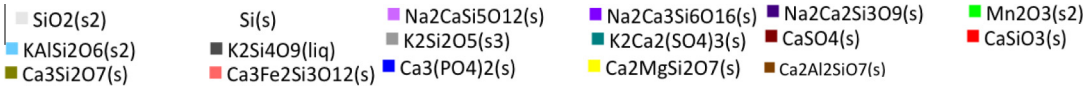

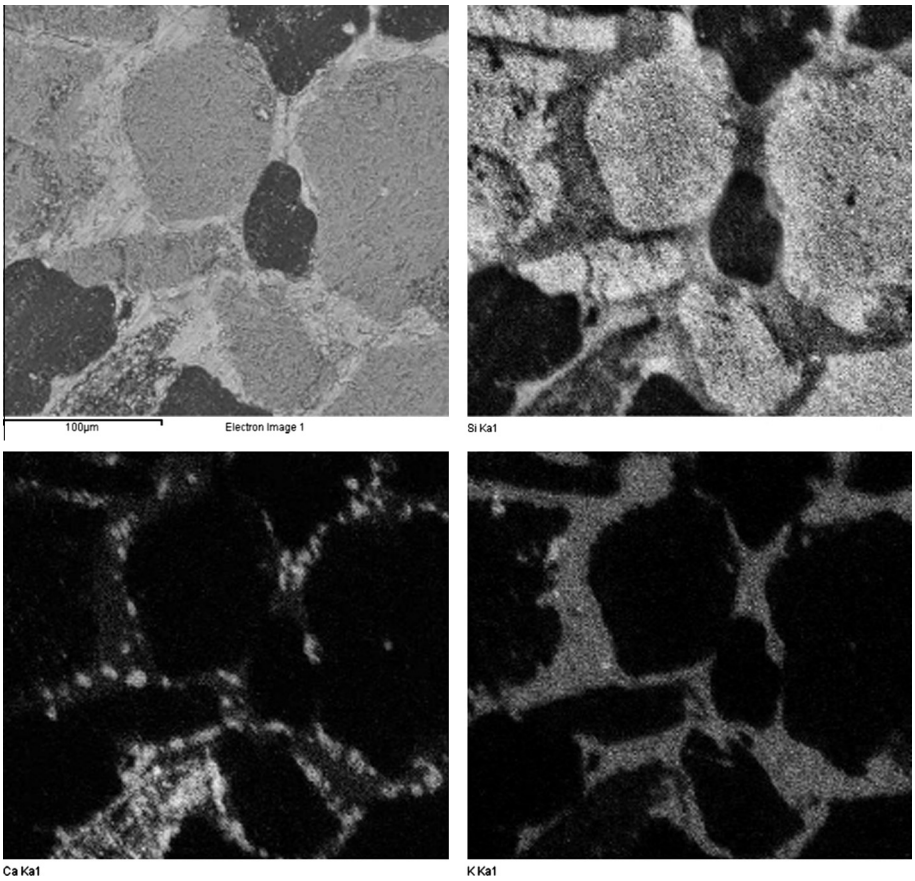

Fig. 17. EDX mapping results for agglomerated bed material seen in Fig. 6B and taken from the particle distributor of the boiler. Upper left: back scattered electron image. Upper right: Si map. Lower left: Ca map Lower right K map.

scale suggest once more that the layer close to the particle is more dense compared to the outer layer forming a more porous layer. The crosses mark the positions where the elemental analyses were performed. The result, presented in Fig. 12, shows that the spots can be divided into three groups based on their elemental composition: the core of the bed particle (quartz), the inner, and the outer ash layer.

The inner ash layer contains 5–7% K, 3–5% Ca, and high concentration of Si (not seen in Fig. 12). The outer layer is rich in Ca (between 25% and 30%) and generally contains lower concentration of K. The concentration of Si remains high, but decreases in favour of Ca. The mean values of the elemental composition in the three groups identified were calculated and used as input data in the thermodynamic equilibrium model.

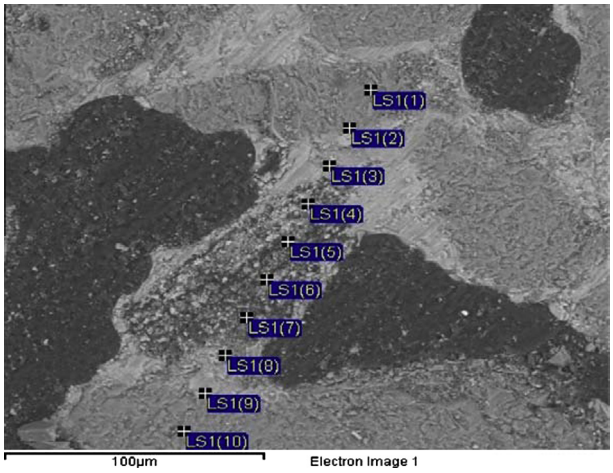

Fig. 18. Bed particle with ash layer of agglomerated bed material seen in Fig. 6B and taken from the particle distributor of the boiler. LS1(1)–LS1(10) is a 10 spots line scan and element composition is shown in Fig. 19.

Fig. 13 shows the predicted composition at 850 °C. The Ca detected in the core group is predicated to be present as $CaSiO_3$. The inner layer is composed of both liquid and solid ash compounds. Potassium is present as liquid $K_2Si_4O_9$ (28%), Na as solid $Na_2Ca_3Si_6O_{16}$, and the remaining Ca as $CaSiO_3$. The elevated concentration of Ca in the outer layer is predicted to be sequestered in $CaSiO_3$ and $CaMgSi_2O_6$, and represents more than 67%. The share of liquid alkali silicate is reduced in the outer ash layer to 18%.

The composition of the quartz core is constant over the entire temperature interval investigated apart from changes in the solid phases of SiO_2 and $CaSiO_3$. The composition of the inner layer is more complex with regard to temperature. Potassium silicate ($K_2Si_4O_9$) is present in solid form up to 750 °C and completely melted above 775 °C. Sodium is thermodynamically stable as solid $Na_2Ca_3Si_6O_{16}$ in the range 600–1125 °C, and as $Na_2CaSi_5O_{12}$ above 1125 °C. The Ca compounds in the outer layer are also thermodynamically stable over the entire temperature interval investigated with the exception of changes in between the solid phases. The stable form of $K_2Si_4O_9$ follows the same pattern as observed for the inner layer.

3.4. Case C: bark pellets and solid recovered fuel

Fig. 14 shows the cross section of a quartz particle covered with ash from the bottom bed sample collected during combustion of bark pellets and solid recovered fuel. The ash layer is composed of ash material, the density of which varies. Fig. 15 shows the elemental compositions in the line scan which starts in the epoxy resin and end in the core of the quartz particle. There are differences in the composition and an inner and outer layer can be identified. A significant amount of Na was found along with K in the part of the ash layer, R1(6)–R1(13), that is richest in alkali metals (5–6% K and 2–3% Na).

Fig. 16 shows the results from the modelled equilibrium composition. The inner ash layer is composed of quartz, $CaSiO_3$, liquid $K_2Si_4O_9$ (18–31 wt.%) and Na present are mainly stable as $Na_2Ca_3Si_6O_{16}$ but also $Na_2CaSi_5O_{12}$ (spot 9). The outer layer is composed of $CaSiO_3$ and $Ca_3Si_2O_7$. Sodium and K present are stable as solid silicates ($K_2Si_2O_5$, $NaCaSi_3O_9$).

3.5. Composition of agglomerates

EDX mapping results are seen in Fig. 17 of the cross-section of the agglomerated bed material seen in Fig. 6B and taken from the particle distributor of the boiler, number 9 in Fig. 3. The EDX mapping results show that the phase binding the particles together is in fact a potassium silicate melt. An interesting detail seen here is that calcium occurs in spots and more or less separate from potassium in the bridging phase between sand particles. This does not resemble what was found for the non-sintered bed material samples where Ca was found to be present in an exterior, continuous phase covering the sand particles and their potassium silicate surface layer. The occurrence of Ca in crystals and not in a continuous phase was verified by further SEM investigations. This data also verified that the Ca-rich crystals were surrounded by K-rich silicate melt.

Fig. 18 shows an enlargement of the agglomerated bed material in Fig. 17, (the bottom left part of Fig. 17). The different shades of grey show that the ash composition varies along the line scan and Fig. 19 shows the element concentrations. The "glue" phase with the lightest colour is clearly richer in K than the other parts of the agglomerate. The concentrations of Ca, Mg and P along this line show that the dark particle is probably an ash particle that has been glued to the sticky sand particles and thus incorporated in the agglomerate.

The results of the thermodynamic equilibrium calculations regarding this case is showed in Fig. 20 and revealed that, in spots containing K, K forms liquid $K_2Si_4O_9$ with one exception, i.e. LS1(7). Apart from liquid $K_2Si_4O_9$, K forms $KAlSi_2O_6$ (LS1(4) and LS1(5)). The presence of Al is a prerequisite. These results are consistent with previous observations presented in this paper. The spots LS1(4)–LS1(7) containing the elements Mg, Ca, P, Al and Fe is a fuel ash particle trapped and glued together in between two quartz ash particles covered with $K_2Si_4O_9$ in liquid form. LS1(3) and LS1(8)

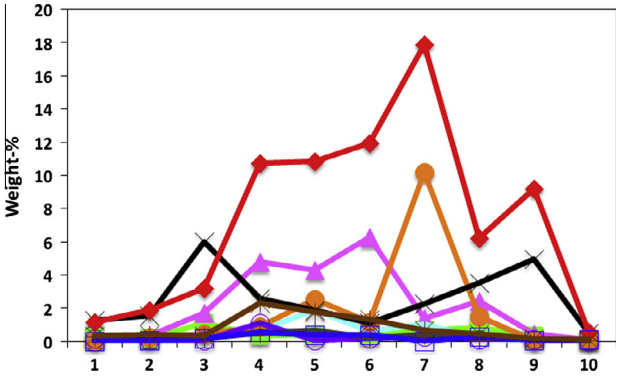

Fig. 19. Elemental concentration (wt.-%) in each spot of the line scan LS1(1)–LS1(10) in Fig. 18. Silicon and oxygen excluded in the plot.

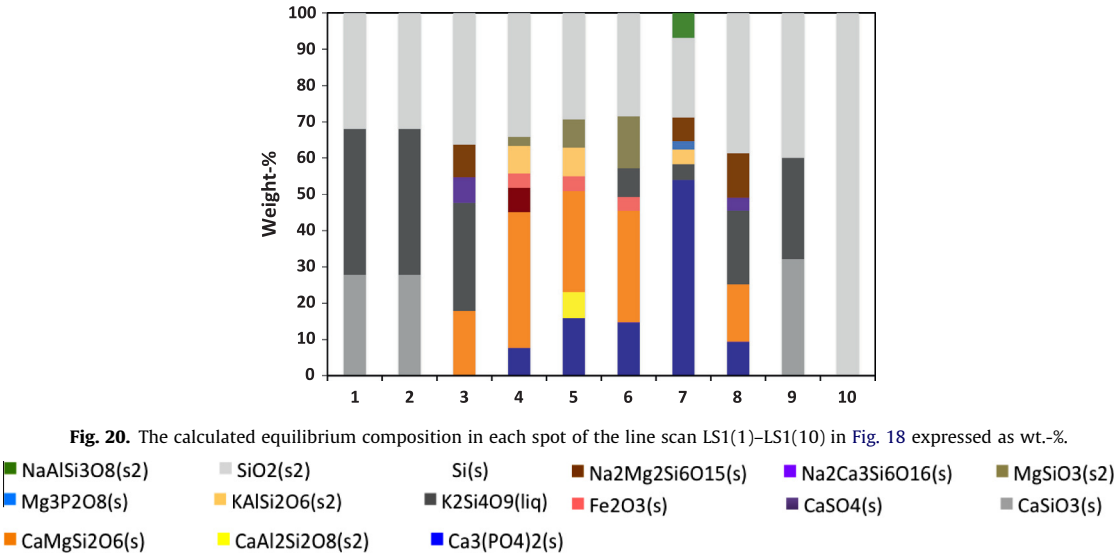

Fig. 20. The calculated equilibrium composition in each spot of the line scan LS1(1)–LS1(10) in Fig. 18 expressed as wt.-%.

show some similarities in the predicted composition as regards to SiO_2, $Na_2Mg_2Si_6O_{15}$, $Na_2Ca_3Si6O_{16}$, $K_2Si_4O_9$, $CaMgSi_2O_6$. These two spots are located on either side of the fuel ash particle.

4. Discussion and Conclusions

Based on the results from test cases A, B and C and the agglomerates collected, the following conclusions can be made:

- The dominant reaction paths in the ash layers formed on silica sand bed material involve the formation of potassium and calcium silicates.
- The characteristic dual ash layer previously reported in the literature [25,26,34,44,46] is confirmed.
- This dual ash layer consists of an inner layer rich in potassium that is potassium silicate and an outer layer rich in calcium where calcium silicate is dominant.
- A scanning electron microscope equipped with an energy dispersive X-ray spectrometer (SEM–EDX) is a powerful tool in analysing bed materials with ash layers and agglomerates from fluidised beds using biomass for the thermal conversion into heat, electricity and fuels for the transportation sector.
- The results using a SEM equipped with an EDX spectrometer can be used as input for thermodynamic equilibrium modelling.
- The results using thermodynamic equilibrium modelling show two important findings:
  (a) The formation of the inner ash layer and potassium silicate in the form of K_2SiO_9 in liquid form. This liquid form of K_2SiO_9 which is also expressed as $K_2O{\cdot}4SiO_2$ in Fig. 2 probably leads to a sticky coating of the quartz sand particles which induce agglomeration if this inner ash layer is not covered by non-sticky ash particles consisting of calcium silicate.
  (b) The formation of the outer ash layer of calcium silicate ($CaSiO_3$) in solid form. This solid form of $CaSiO_3$ is crucial for preventing the development of agglomerates. Lack of a proper layer of calcium silicate, see Fig. 17, was seen in the case of full development of agglomerates found in the particle seal of the boiler.

The build-up of a protective ash layer of calcium silicate can be promoted by either co-combustion of a calcium-rich fuel such as lignite (brown coal), some peat qualities or bark such as in test case C. Limestone can also be added to the combustion chamber of a fluidized bed as in the case when rapeseed cake pellets were co-fired with wood in the Chalmers boiler [38]. Test case A using straw pellets with wood only as base fuel in resulted in too low calcium loading to the boiler and after 96 h of operation severe agglomerates were found in the particle distributor of the boiler, agglomerates illustrated by Fig. 6. Using the phase diagram of the K_2O–CaO–SiO_2 (Fig. 2) as input in the available databases (FTsalt, FToxid, and FACT53, [15]), thermodynamic equilibrium modelling can foresee operating problems related to agglomeration of the bed material in fluidized bed boilers when quartz sand is used. This is true despite the limitations in the predictions of melting temperatures and phase equilibria for the main subsystem in biomass ashes that represents the ternary phase diagram K_2O–CaO–SiO_2 [15]. According to [41] the limitations are the lack of optimization of the phase diagram and that is due to the use of inconsistent data from literature to determine the main parameters in the modelling of the phase diagram by for example the FactSage program. These limitations give a large deviation in the predicted liquidus temperatures compared to the measured ones, 200–400 °C, [41]. In the present paper, it is the liquid form of $K_2Si_4O_9$ that is the basis for the understanding of the sticky nature of the bed particles. Liquid $K_2Si_4O_9$ that is $K_2O{\cdot}4SiO_2$ in the high SiO_2 corner of the phase diagram of the ternary system K_2O–CaO–SiO_2 (Fig. 2) is thermodynamically stable already at a temperature of 750 °C. This prediction is correct in comparison to what can be found in Fig. 2 for $K_2O{\cdot}4SiO_2$. This means that focus should be on the phenomenon that woody biomass ash containing alkali in the form of potassium with insufficient calcium present in combination with the use of quartz sand as bed material can result in the formation of sticky particle coatings at the operating temperatures for fluidized bed reactors used for the thermochemical conversion of biomass.

Advanced thermodynamic equilibrium calculations using SEM–EDX analysis of the coatings of bed material particles is a powerful tool to explain the negative outcome when the boiler has shut down. It is not an on-line method that can be used during the operation of the boiler for supporting bed generation or the addition of limestone or kaolin. Thus other methods are needed in order to prevent agglomeration in full-scale fluidized bed boilers such as the supervision of the particle distributor by a video camera or the measurement of pressure fluctuations in the boiler and/or particle distributor [22,29].

Acknowledgements

This project was financed by Värmeforsk AB (Project: A08-817) and by the Swedish Energy Administration. The practical support

from the operators at Akademiska Hus AB and the research engineers employed by Chalmers University of Technology is also greatly appreciated.

References

[1] Directive 2009/28/EC of the European Parliament and of the Council of 23 April 2009 on the promotion of the use of energy from renewable sources and amending and subsequently repealing directives 2001/77/EC and 2003/30/EC.
[2] Åmand L-E, Leckner B. Metal emissions from co-combustion of sewage sludge and coal/wood in fluidized bed. Fuel 2004;83:1803–21.
[3] Elled A-L, Åmand L-E, Leckner B, Andersson B-Å. The fate of trace elements in fluidised bed combustion of sewage sludge and wood. Fuel 2007;86:843–52.
[4] Elled A-L, Åmand L-E, Eskilsson D. Fate of zinc during combustion of demolition wood in a fluidized bed boiler. Energy Fuels 2008;22:1519–26.
[5] Zhao D, Åmand L-E, Öhlin J, Bohwalli J, Cai R, Zhang YG. Emissions of mercury and cadmium when co-firing municipal sewage and/or waste pellets with biomass in a CFB boiler. In: Proceedings of the 21st international conference on fluidized bed combustion, Naples, Italy June 3–6; 2012.
[6] Yao H, Mkilaha ISN, Naruse I. Screening of sorbents and capture of lead and cadmium compounds during sewage sludge combustion. Fuel 2004;83:1001–7.
[7] Gale T, Wendt JOL. High temperature interaction between multiple-metals and kaolinite. Combust Flame 2002;131:299–307.
[8] Gale TK, Wendt JOL. In-furnace capture of cadmium and other semi-volatile metals by sorbents. Proc Combust Inst 2005;30:2999–3007.
[9] Wendt JOL, Lee SJ. High-temperature sorbents for Hg, Cd, Pb and other trace metals: mechanisms and applications. Fuel 2010;89:894–903.
[10] Åmand L-E, Leckner B, Eskilsson D, Tullin C. Deposits on heat transfer tubes during co-combustion of biofuels and sewage sludge. Fuel 2006;85:1313–22.
[11] Åmand L-E, Leckner B, Lücke K, Werther J. Gaseous emissions from co-combustion of sewage sludge and coal/wood in fluidized bed. Fuel 2004;83:477–86.
[12] Davidsson K, Åmand L-E, Elled A-L, Leckner B. Effect of cofiring coal and biofuel with sewage sludge on alkali problems in a circulating fluidized bed boiler. Energy Fuels 2007;21:3180–8.
[13] Kassman H. Strategies to reduce gaseous KCl and chlorine in deposits during combustion of biomass in fluidised bed boilers. Page 12 and Paper I in Academic Dissertation, Chalmers University of Technology, Göteborg, Sweden; 2012, ISSN 0346–718X.
[14] Miettinen-Westberg H, Byström M, Leckner B. Distribution of potassium, chlorine, and sulfur between solid and vapor phases during combustion of wood chips and coal. Energy Fuels 2003;17:18–28.
[15] Lindberg D, Backman R, Chartrand P, Hupa M. Towards a comprehensive thermodynamic database for ash-forming elements in biomass and waste combustion current situation and future developments. Fuel Process Technol 2013;105:129–41.
[16] Silvennoinen J, Hedman M. Co-firing of agricultural fuels in a full-scale fluidized bed boiler. Fuel Process Technol 2013;105:11–9.
[17] Öhman M, Nordin A, Skrifvars B-J, Backman R, Hupa M. Bed agglomeration characteristics during fluidized bed combustion of biomass fuels. Energy Fuels 2000;14:169–78.
[18] Lin W, Dam-Johansen K, Frandsen F. Agglomeration in bio-fuel fired fluidized bed combustors. Chem Eng J 2003;96:171–85.
[19] Salour D, Jenkins BM, Vafaei M, Kayhanian M. Control of in-bed agglomeration by fuel blending in a pilot scale straw and wood fueled AFBC. Biomass Bioenergy 1993;4:117–33.
[20] Grubor BD, Oka SN, Ilic MS, Dakic DV, Arsic BT. Biomass FBC combustion-bed agglomeration problems. In: Proceeding of the 13th international conference on fluidized bed combustion. New York: ASME; 1995. p. 515–22.
[21] Bapat DW, Kulkarni SV, Bhandarkar VP. Design and operating experience on fluidized bed boiler burning biomass fuels with high alkali ash. In: Proceeding of the 14th international conference on fluidized bed combustion. New York: ASME; 1997, 165–74.
[22] Scala F, Chirone R. Characterization and early detection of bed agglomeration during fluidized bed combustion of olive husk. Energy Fuels 2006;20:120–32.
[23] Scala F, Chirone R. An SEM/EDX study of bed agglomeration formed during fluidized bed combustion of three biomass fuels. Biomass Bioenergy 2008;32:252–66.
[24] Steenari B-M, Åmand L-E, Bohwalli J. Agglomeration of the bed material in fluidized bed reactors for thermal conversion of biomass – a threat for the development of the technology. In: Joint meeting Swedish-Finnish Flame Days and the Scandinavian – Nordic Section of the Combustion Institute, January 26–27, Piteå, Sweden; 2011.
[25] Nuutinen LH, Tiainen M, Virtanen ME, Enestam SH, Laitinen RS. Coating layers on bed particles during biomass fuel combustion in fluidized-bed boilers. Energy Fuels 2004;18:127–39.
[26] Öhman M, Pommer L, Nordin A. Bed agglomeration characteristics and mechanisms during gasification and combustion of biomass fuels. Energy Fuels 2005;19:1742–8.
[27] Zevenhoven-Onderwater M, Öhman M, Skrifvars B-J, Backman R, Nordin A, Hupa M. Bed agglomeration characteristics of wood-derived fuels in FBC. Energy Fuels 2006;20:818–24.
[28] De Geyter S, Öhman M, Boström D, Eriksson M, Nordin A. Effects of non-quarts minerals in natural bed sand on agglomeration characteristics during fluidized bed combustion of biomass fuels. Energy Fuels 2007;21:2663–8.
[29] Bartels M, Lin Weigang, Nijenhuis J, Kapteijn F, van Ommen JR. Agglomeration in fluidized beds at high temperatures: Mechanisms, detection and prevention. Prog Energy Combust Sci 2008;34:633–66.
[30] Carter CB, Norton MG. In ceramic materials: science and engineering. New York: Springer; 2007, ISBN 978-0-387-46270-7. pp. 139–442.
[31] Skrifvars BJ, Hupa M, Backman R, Hiltunen M. Sintering mechanisms in FBC ashes. Fuel 1994;73:171–6.
[32] Olofsson G, Ye Zhicheng, Bjerle I, Andersson A. Bed agglomeration problems in fluidized-bed biomass combustion. Ind Eng Chem Res 2002;41:2888–94.
[33] Brus E, Öhman M, Nordin A. Mechanisms of bed agglomeration during fluidized-bed combustion of biomass fuels. Energy Fuels 2005;19:825–32.
[34] De Geyter S. Measures for preventing bed agglomeration using ash reaction chemistry. Licentiate Thesis ISBN 978-91-7264-707-7, 2008, Umeå University, Umeå, Sweden.
[35] Visser HJM, van Lith SC, Kiel JHA. Biomass ash-bed material interactions leading to agglomeration in FBC. J Energy Res Technol 2008;130. 011801-1-011801-6.
[36] Piotrowska P, Grimm A, Skoglund N, Boman C, Öhman M, Zevenhoven M, et al. Fluidized bed combustion of mixtures of rapeseed cake and bark: the resulting bed agglomeration characteristics. Energy Fuels 2012;26:2028–37.
[37] Davidsson KO, Åmand L-E, Steenari B-M, Elled A-L, Eskilsson D, Leckner B. Countermeasures against alkali-related problems during combustion of biomass in a circulating fluidized bed boiler. Chem Eng Sci 2008;63:5314–29.
[38] Piotrowska P, Zevenhoven M, Davidsson K, Hupa M, Åmand L-E. Fate of alkali metals and phosphorous of rapeseed cake in circulating fluidized bed boiler part 1: cocombustion with wood. Energy Fuels 2010;24:333–45.
[39] Grimm A, Skoglund N, Boström D, Öhman M. Bed agglomeration characteristics in fluidized quartz bed combustion of phosphorous-rich biomass fuels. Energy Fuels 2011;25:937–47.
[40] Barisic V, Åmand L-E, Coda Zabetta E. The role of limestone in preventing agglomeration and slagging during CFB combustion of high-phosphorous fuels. In: Proceeding of the poster session of World BioEnergy 2008 Conference & Exhibition on Biomass for Energ, Jönköping Sweden; 2008. pp. 259–63.
[41] Berjonneau J, Colombel L, Poirier J, Pichavant M, Defoort F, Seiler J. Determination of liquidus temperatures of ashes from biomass gazification for fuel production by thermodynamical and experimental approaches. Energy Fuels 2009;23:6231–41.
[42] Steenari B-M, Lindqvist O. High-temperature reactions of straw ash and the anti-sintering additives kaolin and dolomite. Biomass Bioenergy 1998;14:67–76.
[43] Tran KQ, Iisa K, Steenari B-M, Lindqvist O. A kinetic study of gaseous alkali capture by kaolin in the fixed bed reactor equipped with an alkali detector. Fuel 2005;84:169–75.
[44] Fernández Llorente MJ, Díaz Arocas P, Gutiérrez Nebot, Carrasco García JE. The effect of the addition of chemical materials on the sintering of biomass ash. Fuel 2008;87:2651–8.
[45] Brus E, Öhman M, Nordin A, Boström D, Hedman H, Eklund A. Bed agglomeration characteristics of biomass fuels using blast-furnace slag as bed material. Energy Fuels 2004;18:1187–93.
[46] Pommer L, Öhman M, Boström D, Burvall J, Backman R, Olofsson I, et al. Mechanisms behind the positive effect on bed agglomeration and deposit formation combusting forest residue with peat additives in fluidized beds. Energy Fuels 2009;23:4245–53.
[47] Wu P, Eriksson G, Pelton AD. Optimization of the thermodynamic properties and phase-diagrams of the Na_2O–SiO_2 and K_2O–SiO_2 systems. J Am Ceram Soc 1993;76:2059–64.
[48] Zevenhoven-Onderwater M, Blomquist JP, Skrifvars B-J, Backman R, Hupa M. The prediction of behaviour of ashes from five different solid fuels in fluidised bed combustion. Fuel 2000;79:1353–61.
[49] Zevenhoven-Onderwater M, Backman R, Skrifvars B-J, Hupa M. The ash chemistry in fluidized bed gasification of biomass fuels. Part I: predicting the chemistry of melting ashes and ash-bed material interaction. Fuel 2001;80:1489–502.
[50] Zevenhoven-Onderwater M, Backman R, Skrifvars B-J, Hupa M, Rosén LiliendahlT, et al. The ash chemistry in fluidized bed gasification of biomass fuels. Part II: ash behavior prediction versus bench scale agglomeration tests. Fuel 2001;80:1503–12.
[51] Risnes H, Fjellerup J, Henriksen U, Moilanen A, Norby P, Papadakis K, et al. Calcium addition in straw gasification. Fuel 2003;82:641–51.
[52] Morey GW, Kracek FC, Bowen NL. The ternary system K_2O–CaO–SiO_2. J Soc Glass Technol 1930;14:158.
[53] Grimm A, Öhman M, Lindberg T, Fredriksson A, Boström D. Bed agglomeration characteristics in fluidized-bed combustion of biomass fuels using olivine as bed material. Energy Fuels 2012;26:4550–9.